Assembly of Complement Components C5b-8 and C5b-9 on Lipid Bilayer Membranes: Visualization by Freeze-Etch Electron Microscopy†

Michael A. McCloskey,*,§,‖ John R. Dankert,‡ and Alfred F. Esser*,‡
Department of Physiology and Biophysics, University of California, Irvine, California 92717, and Department of Comparative and Experimental Pathology, University of Florida, Gainesville, Florida 32610
Received April 14, 1988; Revised Manuscript Received August 16, 1988

ABSTRACT: We have visualized by freeze-etch electron microscopy the macromolecular complexes of complement, C5b-8 and C5b-9, respectively, assembled on synthetic phospholipid bilayers. These complexes were formed sequentially by using purified human complement components C5b-6 followed by C7, C8, and C9. Complexes of C5b-8 were observed on the external surface (ES) of vesicles as 12-nm particles that tended to form polydisperse aggregates. The aggregates were sometimes of a regular chainlike structure containing varying numbers of paired subunits. Etching of vesicles containing C5b-9 complexes revealed on the ES large rings of ≈27-nm outer diameter. One or two knobs usually were attached to the perimeter of the rings. Splitting of the membrane resulted in partitioning of the C5b-9 with the outer leaflet. Thus, round holes of ≈17-nm diameter were present in the protoplasmic face (PF), and raised circular stumps of a matching size were present on the exoplasmic face (EF) of C5b-9 vesicles. C5b-9 complexes were frequently localized in regions of the lowest lipid order. That is, in micrographs of the EF and ES, single C5b-9 complexes were located where the ripples of the $P_{\beta'}$ phase bend or reach a dead end, and linear arrays of C5b-9 complexes outlined disclination-like structures in the lattice; the holes in the PF mirrored this distribution. The membrane immediately surrounding C5b-9 rings was often sunk inwardly over an area much larger than that of the ring itself. Thus, shallow depressions were seen about the rings on the ES and around the holes in the PF, whereas raised areolas surrounded the stumps on the EF. These areolas presumably were composed of lipid because of their rippled appearance characteristic of the $P_{\beta'}$ phase. These observations are consistent with the hypothesis that the C5b-9 complex is capable of restructuring lipid organization in its immediate environment and that such an effect may participate in the mechanism whereby complement permeabilizes cell membranes.

The precise mechanism by which the membrane attack complex of complement (MAC)[1] impairs cell membrane function is not yet resolved. Since its formulation in 1972 the pore or "doughnut" hypothesis of Mayer (1972) has enjoyed wide popularity. The gist of this model is that the MAC, or C5b-9 protein complex, forms a central aqueous pore that spans the bilayer and allows rapid transmembrane exchange of salts and water. Early support for the doughnut hypothesis came from negative-stain electron micrographs (EM) of complement-lysed erythrocytes, which show accumulations of stain in dark circular areas of 9-13-nm diameter. Freeze-etch EM of the same system also reveals doughnut-like projections on the external membrane surface and proteinaceous stubs projecting from the hydrophobic fracture face of the outer monolayer (Iles et al., 1973; Bhakdi et al., 1974; Tranum-Jensen & Bhakdi, 1983).

More recent support for the doughnut hypothesis comes from the finding that under certain conditions, e.g., high temperature or the presence of heavy metals or exogenous proteases, purified complement component C9 forms a tubular structure composed of 12-18 C9 protomers (Podack & Tschopp, 1982; Tschopp et al., 1984). The tube has an annulus at one end such that the external dimensions are ≈21 × 15 × 15 nm (DiScipio & Hugli, 1985). This structure, termed poly(C9), is presumably responsible for the classical doughnut-like appearance of C5b-9 in negative-stain and freeze-fracture electron micrographs of complement-treated erythrocytes. It has been suggested that poly(C9) forms the hypothetical pore of Mayer's model (Tschopp et al., 1982). Recent evidence indicates, however, that poly(C9) formation is not a requirement for hemolysis (Dankert & Esser, 1985) or bacterial killing (Dankert & Esser, 1987).

An alternative to the doughnut hypothesis is the so-called "leaky-patch" model (Lachmann et al., 1970; Hesketh et al., 1971; Kinsky, 1972; Esser et al., 1979a). In this model the membrane lipids in an area surrounding the MAC are reorganized to the extent of being leaky to solutes and water. Some spin-label work suggests that complement proteins C5b-8 and C5b-9 may indeed perturb the packing of lipids in planar bilayers (Esser et al., 1979b). Previous freeze-etch studies of complement-treated erythrocyte membranes have not revealed a structural basis for the spin-label data, but it is quite possible that the very high density of endogenous proteins in this system would obscure such effects. One goal of the present study was to use freeze-etch EM to explore possible effects of the MAC on bilayer structure in vesicles lacking all protein save the complement proteins themselves.

A secondary concern with previous EM studies of the MAC is whether formation of the classical complement ring structure is an artifact of experimental protocol. Trypsin and/or negative stains have been used to visualize the rings, yet we know

† This research was supported by grants from the NIH to M.A.M. (GM 35901), J.R.D. (AI 22912), and A.F.E. (AI 19478).
* Address correspondence to either author.
§ University of California.
‖ Present address: Department of Biological Sciences, Columbia University, New York, NY 10027.
‡ University of Florida.

[1] Abbreviations: DNP, 2,4-dinitrophenyl; DPPC, dipalmitoylphosphatidylcholine; EF, exoplasmic fracture face; EM, electron microscopy or electron micrographs; ES, exoplasmic (or external) surface; IMPs, intramembranous particles; MAC, membrane attack complex of complement; PF, protoplasmic fracture face.

0006-2960/89/0428-0534$01.50/0

that proteases and certain metals induce polymerization of C9 (Dankert et al., 1985). In their freeze–etch study Tranum-Jensen and Bhakdi (1983) examined nontrypsinized ghosts and found that "the extramembrane annuli of complement lesions were visualized clearly only in preparations of proteolytically stripped membranes". In fact, even their nontrypsinized membranes were unintentionally exposed to proteases that are generated by activation of serum complement and the clotting and fibrinolytic systems. Tschopp et al. (1984) presented scanning-transmission EM photos of unstained, heat-polymerized C9, but these micrographs do not reveal a ring or a pore structure. It thus remains to be shown unequivocally that the ring structure is formed during assembly of the MAC in the absence of proteases or negative stains.

Here we present freeze–etch electron micrographs of the hemolytic C5b-8 and C5b-9 complexes assembled on vesicles composed of synthetic phospholpids. This simplified system has permitted us to identify membrane-associated C5b-8 complexes in the form of ordered and irregular oligomers. It has also revealed a striking effect of the C5b-9 complex on the surrounding lipid phase. The C5b-9 complex itself appears to span the bilayer. Finally, our results confirm the assumption that formation of the doughnut-shaped MAC is not an artifact of proteolysis or negative staining. A preliminary account of this work has appeared (McCloskey et al., 1986).

Materials and Methods

Lipids. Dipalmitoylphosphatidylcholine (DPPC), *N*-(7-nitro-2,1,3-benzoxadiazol-4-yl)phosphatidylethanolamine (NBD-PE), and 1-palmitoyl-2-oleoylphosphatidylserine (PO-PS) were purchased from Avanti (Birmingham, AL). 2,4-Dinitrophenyl (DNP) gangliosides were prepared from beef brain gangliosides (Supelco, Bellefonte, PA) as described previously (McCloskey & Poo, 1986).

Proteins. Complement proteins C5b-6, C7, C8, and C9 were isolated as described by Esser and Sodetz (1988). Rabbit anti-DNP BSA was purchased from Miles Scientific (Naperville, IL) and purified further by affinity chromatography on a column containing (trinitrophenyl)lysine coupled to agarose. The antibody was eluted with 20 mM (trinitrophenyl)lysine in borate-buffered saline, pH 8.0.

Vesicle Formation. Large unilamellar and oligolamellar phospholipid vesicles were formed essentially as described by Reeves and Dowben (1969). A mixture containing 2.5 μmol of total lipid was dissolved in 3 mL of $CHCl_3$–CH_3OH (1:1 v/v) and the solution applied to a large Petri dish (14-cm diameter). The solvent was evaporated by floating the dish on a water bath at 10–20 °C above the melting point of the highest melting lipid; the plate was rocked during solvent removal to form as even a lipid film as possible. After the solvent had evaporated, the plate was kept in a moist chamber for 30 min at room temperature, after which time 30 mL of 0.320 M sucrose was added. The plate was covered with Saran Wrap and aluminum foil and floated overnight on a water bath at 10–20 °C above the melting point of the lipid. The lipid suspension was then diluted with an equal volume of 0.320 M glucose (to reduce the density of the medium) and centrifuged at 20000*g* for 30–45 min. The pellet was resuspended in 0.320 M sucrose and the suspension passed through 0.4-μm pore-size Nucleopore polycarbonate membranes (Pleasanton, CA) to decrease the vesicle size (Szoka et al., 1980). Vesicles were then rinsed by suspension in 10 mM Tris and 145 mM NaCl (pH 7.2) and centrifugation for 20 min in an Eppendorf microcentrifuge, resuspended in the same buffer at approximately 2 μmol/mL, and used as described below. The lipid composition of the vesicles shown in Figures 2–7 was DPPC:POPS:DNP gangliosides:NBD-PE (91.5:7.5:0.5:0.5 mol %).

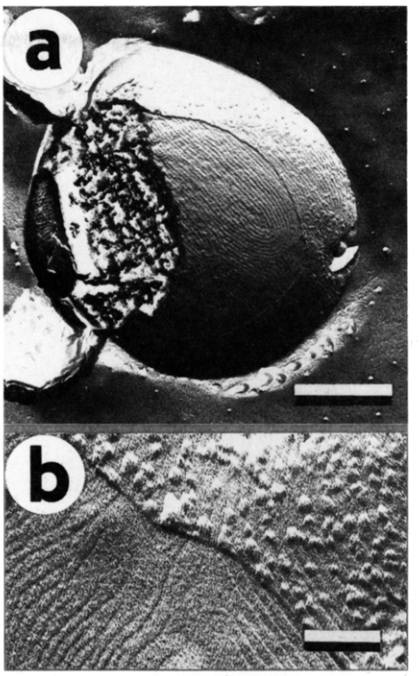

FIGURE 1: Visualization of anti-DNP IgG bound to the external surface of freeze–etched DPPC vesicles containing 1 mol % DNP gangliosides. Note clean distinction between ES and PF: Antibody decorates ES, and PF is free of spurious perforations or IMPs. Pt shadow cast from bottom of photo in these and subsequent figures. (A) Magnification = 315000×; bar = 4000 nm. (B) Separate experiment, magnification = 100000×; bar = 100 nm.

Sample Preparation. Vesicles (1 mL) were mixed with 25 μg of C5b-6 and incubated with gentle shaking for 5 min at 37 °C. C7 (50 μg) and C8 (100 μg) were then added at 15-min intervals, and incubation was continued for another 15 min. The sample was split into two aliquots and centrifuged as described above. One portion was resuspended in a volatile buffer (0.1 M ammonium acetate, 0.05 M ammonium bicarbonate, pH 7.4) and used as C5b-8 vesicles; the other aliquot was resuspended in Tris-buffered saline and incubated with 200 μg of C9 and gentle shaking for 30 min at 37 °C. The vesicles carrying C5b-9 were then resuspended in the volatile buffer. Small aliquots from both samples (≈50% suspension of pellet, v/v) were then placed on gold planchets and frozen by dipping them into liquid Freon 22.

Freeze–Etch Electron Microscopy. Vesicle suspensions frozen on gold planchets were fractured with a razor blade at a nominal stage temperature of −101 °C in a Balzers BAF 301 unit (Nashua, NH). Etching was carried out for periods of 3–4.5 min at a pressure of 4×10^{-7} Torr. With the aid of a quartz crystal film thickness monitor a layer (≈2 nm) of Pt/C was deposited from an angle of 45° and the replica then stabilized by deposition of ≈20 nm of carbon. Replicas were floated off the sample onto water, and the residual sample was dissolved by treatment of the replica with 2.5% sodium hypochlorite for 12 h. Replicas were rinsed copiously in distilled water, picked up on 100-mesh Cu grids, dried, and examined in a Zeiss EM-10CR electron microscope at 60 kV. All micrographs are presented such that the platinum deposit is on the bottom edge of the particles.

Results

Labeling of the Exoplasmic Surface. In initial experiments we established the integrity and orientation of the vesicle membranes in our etched preparations. This was done by

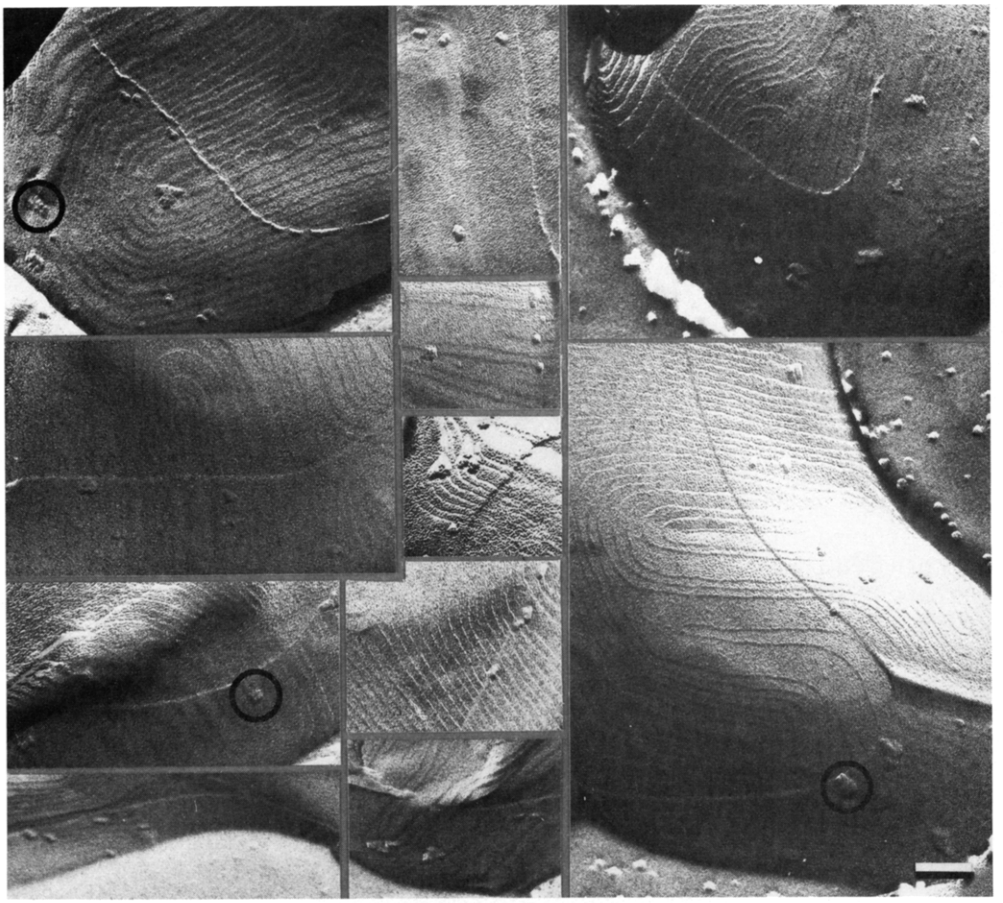

FIGURE 2: Heterogeneous particles on the external surface of freeze–etched vesicles bearing C5b-8. Micrographs are combined from three experiments. Note that aggregates sometimes are regular in structure (circles), with pairs of 12-nm subunits aligned in a row. Magnification = 75000×; bar = 100 nm.

selectively labeling the exoplasmic surface (ES) with rabbit anti-DNP antibodies. The antibodies were bound to DPPC vesicles containing 1 mol % of DNP gangliosides for 60 min at room temperature in the absence of complement. The vesicles were then rinsed once in Tris–NaCl buffer and once in the volatile buffer and finally resuspended in the volatile buffer and quenched from room temperature in liquid Freon. Samples were then processed and the replicas examined in the electron microscope as described under Materials and Methods.

Figure 1 shows images of such replicas at two different magnifications. These micrographs demonstrate three relevant points. First, the protoplasmic fracture face (PF) is neither decorated with intramembranous particles (IMPs) nor perforated with holes; therefore, any such particles or holes that appear after MAC addition must be due to MAC proteins themselves. Second, the etch patterns of the ice surfaces outside and inside the vesicles are markedly different because the 0.32 M sucrose that fills the vesicles forms a nonvolatile eutectic phase. Third, by preparing vesicles from DPPC, we can take advantage of the rippled surface texture characteristic of saturated phosphatidylcholines in the P_{β}' solid phase in analyzing protein–lipid interactions.[2] In control experiments, etching of fractured vesicles not exposed to anti-DNP antibodies revealed an ES devoid of particles, indicating that in our system etching did not generate artifactual particles on the ES of complement-free vesicles.

Freeze–Etch of Vesicles with Assembled C5b-8. Etching of fractured C5b-8 vesicles consistently revealed heterodisperse aggregates of particles on the ES, the smallest subunit of which was 12 ● 1 nm in diameter (Figure 2). Single 12-nm particles coexisted with the lumpy aggregates, and we assume that the monomeric 12-nm particles are the 12-nm subunits of the aggregates. Sometimes the nodular aggregates were amorphous and at other times they appeared ordered, with 2–8 paired subunits aligned in a chain (Figure 2, circles).

It should be noted that the PF of vesicles bearing C5b-8 was devoid of IMPs (Figures 2 and 3), but shallow dimples occasionally could be observed in the PF (Figure 3). These depressions may be complementary to the protrusions visible on the exoplasmic fracture face (EF) (Figure 3), although the chemical nature of the protrusions is unclear.

Freeze–Etch EM of Vesicles with Assembled C5b-9. Large ring- or doughnut-like structures were present on the ES of C5b-9 vesicles (Figures 4 and 5). These structures had an outer diameter of 27 ± 3 nm and a central pit ≈9 nm in diameter.[3] One or two ≈10-nm appendages often protruded from the periphery of these rings. The rings were often localized at bends or ends in the P_{β}' ripples and at defects in the lipid lattice.

[2] At temperatures between the pretransition and the chain melting transition of saturated phosphatidylcholines, the bilayer exists in a solid phase, which exhibits a periodic wave or ripple pattern. The appearance of such ripples in freeze–fracture micrographs indicates the presence of this intermediate state, termed P_{β}' phase by X-ray crystallographers (Luzzati & Tardieu, 1974).

[3] The outer diameter of C5b-9 complexes was measured normal to the direction of the platinum shadow to minimize contributions of the metal coat to the measurement. Nevertheless, the latter was unavoidably an overestimate. The greater apparent size of the C5b-9 rings in this work may also derive from the fact that we did not treat the C5b-9 complex with trypsin or other proteases, as has been done in previous studies to enhance visualizaton or promote assembly of the rings.

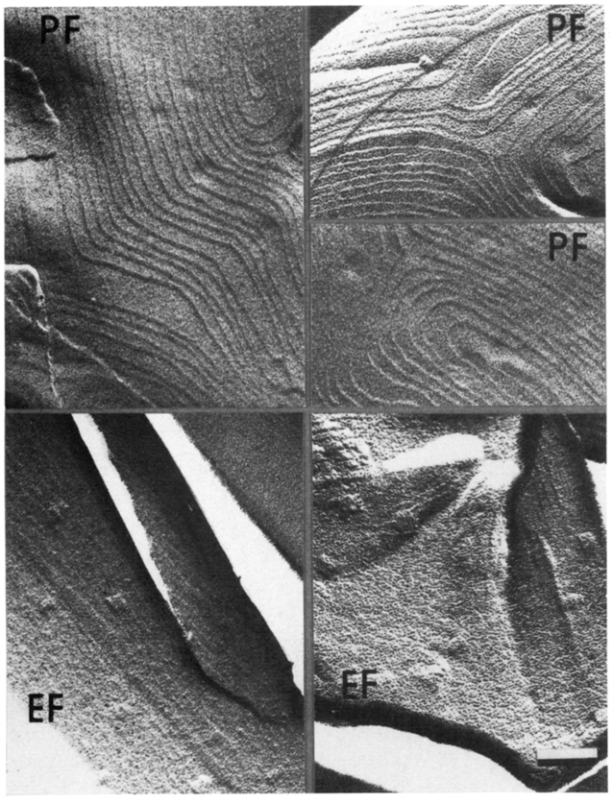

FIGURE 3: Alteration in the hydrocarbon core of freeze–etched C5b-8 vesicles. Dimples are apparent in the PF and warts in the EF. Magnification 80000×; bar = 100 nm.

The PF of etched vesicles containing C5b-9 was perforated with holes of 17 ± 5 nm diameter (Figures 4–6). Round stubs of 16 ± 3 nm outer diameter protruded from the EF of C5b-9 vesicles (Figure 7). Thus, upon splitting of the membrane the MAC partitioned with the outer leaflet, leaving behind holes in the PF and proteinaceous projections on the EF. As described above for rings on the ES, the holes in the PF and the projections from the EF were often localized at bends or dead ends in the $P_{\beta'}$ ripples. These results are consistent with the possibility that all three structures represent different views of the C5b-9 complex.

Remarkably, the area surrounding C5b-9 complexes was often disturbed for distances of several hundred angstoms away from the complex itself. This disturbance was most evident on the EF as a raised areola about the stubs, with an average area of ≈2900 nm^2 (Figure 7). It also was manifest on the ES as a shallow depression framing the doughnuts (Figure 4) and on the PF as a depression centered on the holes (Figures 4 and 6). Nevertheless, not all the C5b-9 complexes were surrounded by a raised area (see, e.g., Figure 4). Even in the absence of complement the membrane of some vesicles had an irregular surface texture, but "warping" of the membrane by the complex was superposed on and distinct from this phenomenon (see, e.g., Figure 6).

Discussion

We have used freeze–etch electron microscopy to visualize the final two stages of MAC assembly on phospholipid bilayers. Freeze–fracture EM provides direct views of membranous proteins from within the hydrophobic interior of the

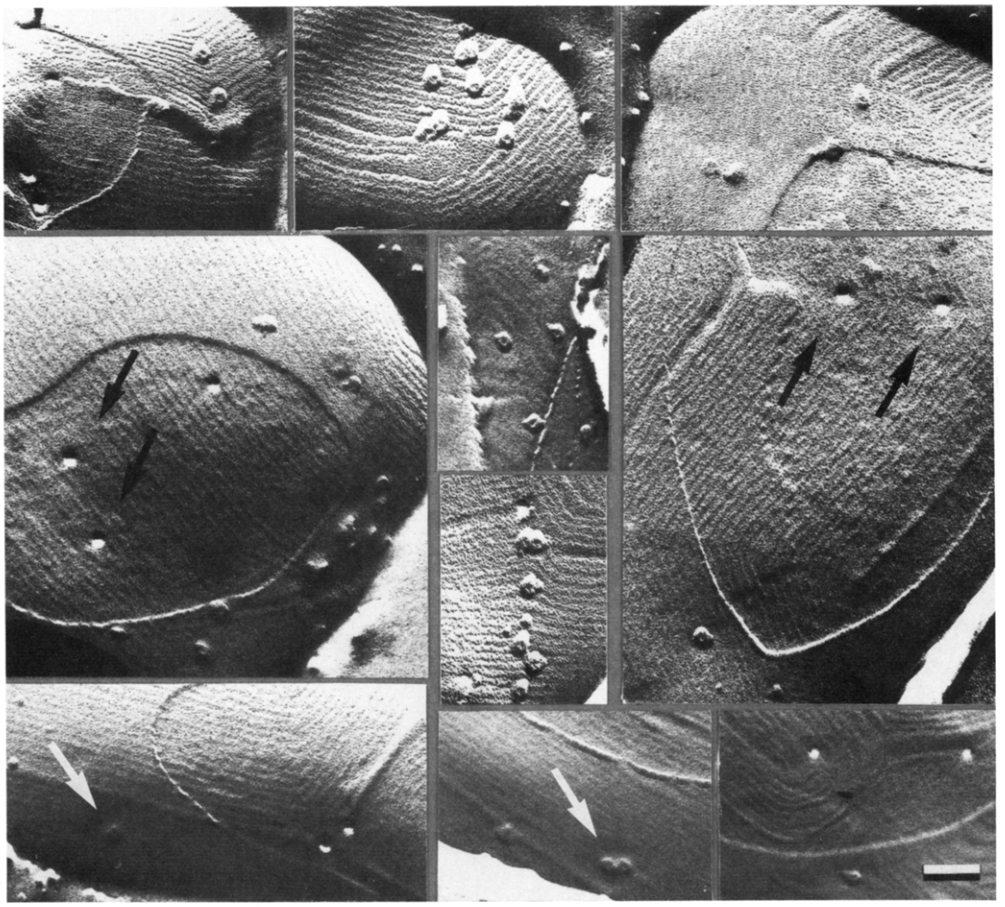

FIGURE 4: Freeze–etch of C5b-9 vesicles. Rings of ≈27-nm diameter are present on the ES, and holes are present in the PF of the same vesicles. Note that the rings and holes often are localized in defect regions of the $P_{\beta'}$ phase. Also, some rings (white arrows) and holes (black arrows) are surrounded by a depressed area of the membrane, the depressions around the holes being less marked. Knobs ≈10 nm in diameter protrude from the edge of many of the rings, and the heterogeneous aggregates present on the ES of C5b-8 vesicles are not in evidence. Magnification = 75000×; bar = 100 nm.

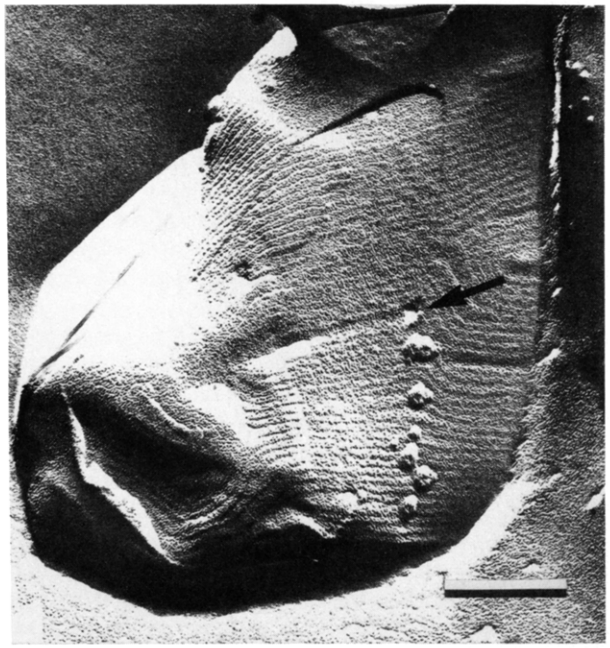

FIGURE 5: View of an entire vesicle bearing a linear array of complexes on the ES (shown as excerpt in Figure 4). Note that array is localized along a disclination-like structure and that where the array of rings reaches the fracture plane a hole (arrow) is present in the PF. Magnification = 80000×; bar = 200 nm.

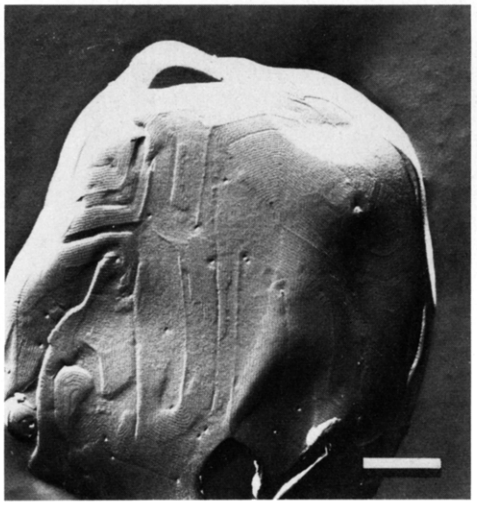

FIGURE 6: Holes in the PF of a single freeze–etched vesicle bearing C5b-9 complexes. Note that holes are often localized at bends or dead ends in the P_{β}' ripples. Magnification = 25200×; bar = 400 nm.

membrane, and freeze–etch EM further reveals the projections of such molecules from the hydrophilic membrane surface.[4] Because of the thickness of the metal coat used to replicate freeze–fractured specimens, detailed information on the substructure of protein complexes such as the MAC is not accessible. For example, it is impossible to determine whether the MAC actually delimits a continuous central pore.[5] Nevertheless, both methods do provide direct information on the structure of the lipid phase, and this information is difficult or impossible to obtain through biochemical or transmission EM studies.

There have been three previous freeze–fracture studies of the MAC, all of them performed on erythrocytes or erythrocyte ghosts (Iles et al., 1973; Bhakdi et al., 1974; Tranum-Jensen & Bhakdi, 1983). We chose to use synthetic lipid vesicles because, unlike the protein-rich erythrocyte membrane, the vesicles lack endogenous proteins and IMPs. This choice allowed us to visualize for the first time via freeze–etch EM the membrane-associated C5b-8 complex. It also permitted resolution of a remarkable effect of the C5b-9 protein complex on the lipid phase. In contrast to previous freeze–fracture studies of the MAC, we also found that trypsinization was not required to visualize MAC doughnuts on the external face of lipid vesicles.

The question of how C5b-8 is organized within or on the membrane is significant because this complex is thought to promote or catalyze assembly of poly(C9) on the membrane and also has hemolytic activity (Gotze et al., 1968; Stolfi, 1968; Haxby et al., 1969; Hesketh et al., 1971; Sims, 1984). It was found in earlier experiments that C5b-8 produces marked changes in the electron paramagnetic resonance spectra of spin labels located in the hydrocarbon region (Esser et al., 1979b) and that $C8_{\alpha-\gamma}$ within this complex is accessible to photoreactive lipids located in the hydrophobic core (Hu et al., 1981; Podack et al., 1981; Steckel et al., 1983). In the present study we did not find discrete IMPs on the hydrophobic fracture faces of C5b-8 vesicles, although subtle alterations of the membrane curvature were evident on the EF and PF of some C5b-8 vesicles (Figure 3). Future studies using the label–fracture method (da Silva & Kan, 1984) may help determine the relationship of these dimples to sites of C5b-8 deposition on the vesicle surface.

C5b-8 was present in the form of large particles of heterogeneous size on the external surface of the lipid vesicles. Coexisting with monomeric 12-nm particles were ordered and irregular aggregates composed of these or similarly sized particles. Most of the mass of the C5b-8 complex was seen exterior to the membrane. In previous negative-stain EM studies of the interaction of terminal complement components with vesicles composed of synthetic lipids, it was suggested that both C5b-7 and C5b-8 form multimeric complexes (Podack et al., 1980). Subsequent fluorescence energy transfer measurements of membrane-bound C8 also indicated that the C5b-8 complex may be polymerized into clusters (Cheng et al., 1985). These multimers of C5b-8 may be related to the ordered chainlike structures we observed on some of the C5b-8-treated vesicles. Neither the regular nor the disordered particle aggregates were prevalent on C9-treated membranes, in agreement with earlier findings (Podack et al., 1980) that addition of C9 leads to dispersal of aggregated C5b-8.

The C5b-9 complexes must extend very deeply into the inner leaflet of the bilayer because of the existence of well-demarcated round holes in the inner leaflet. These holes presumably are created by removal of the proteinaceous stump found in the outer leaflet upon membrane fracture. It might be argued that the hole is due to removal from the inner leaflet of lipids that are tightly bound to the C5b-9 complex, but this seems unlikely in view of the fact that on etched preparations the round stub on the EF has a pronounced pit in its center, suggesting that it is not covered by a slab of lipid derived from the protoplasmic leaflet. Although we did not visualize the protoplasmic surface in any of our replicas, the simplest interpretation of our data is that the MAC fully traverses the vesicle bilayer. Tranum-Jensen and Bhakdi (1983) found that

[4] For useful description of freeze–fracture methodology see Rash and Hudson (1979).

[5] It is also impossible to determine from negative-stain EM whether the large MAC "pore" is actually open or reaches a bottleneck somewhere inside the complex. Negative-stain EM of the acetylcholine receptor [see, e.g., Fairclough et al. (1983)] also reveals a central pit, yet its diameter is much larger that of the ion channel (≈7 Å) as determined from the channel's unitary conductance.

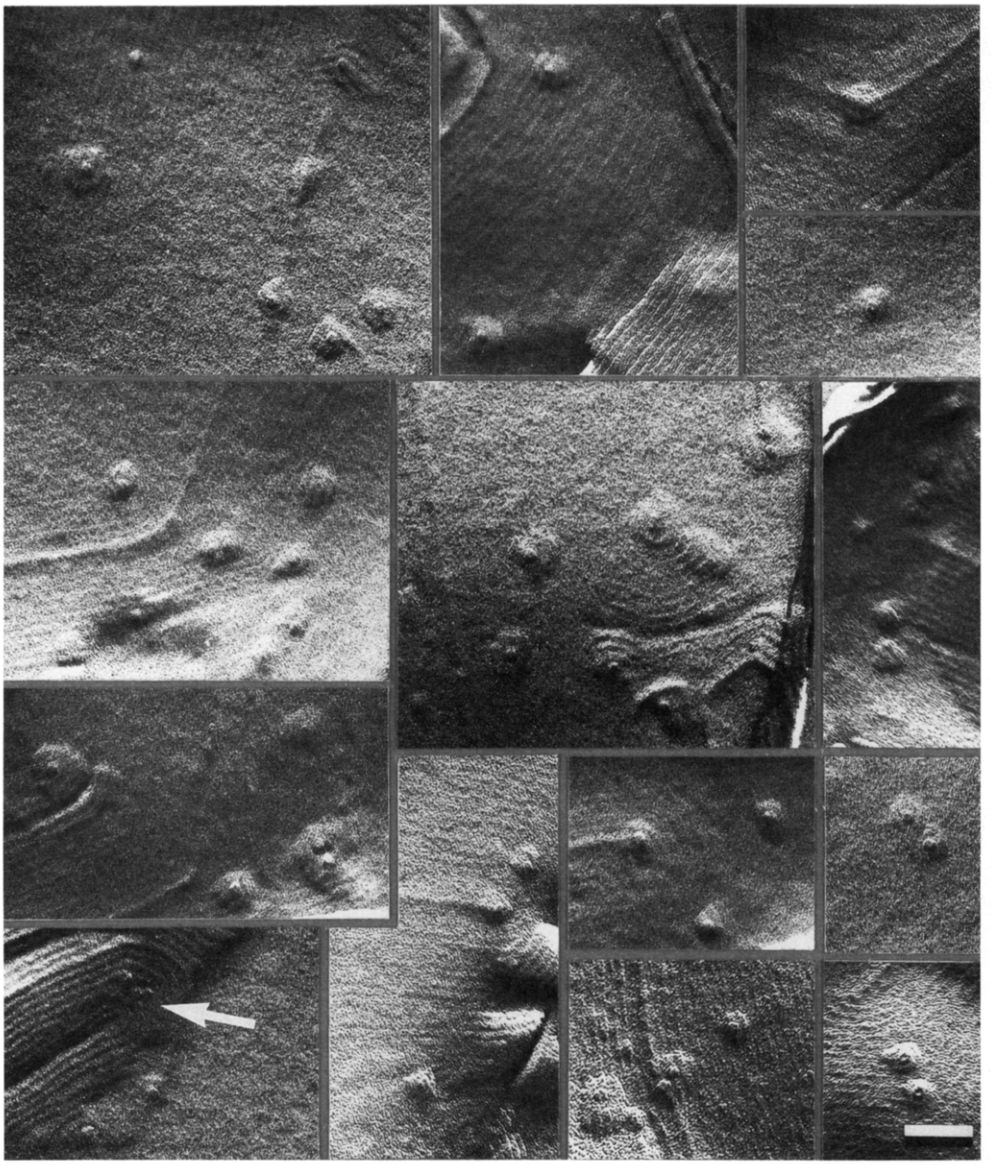

FIGURE 7: Raised areolas surrounding the projection of C5b-9 onto the EF. The diameter of these structures was ≈610 ± 160 Å. Note that, as with the holes in the PF, the stubs with surrounding mesas are often localized in the most disordered regions of the bilayer. Also, the ripples of the $P_{\beta'}$ lipid phase pass directly through many of the areolas, suggesting that the latter are composed primarily of lipid. As indicated by the arrow in the lower left corner, some C5b-9 complexes are not surrounded by areolas on the EF. Magnification = 90000×; bar = 100 nm.

C5b-9 creates holes or "pits" in the inner leaflet of freeze–etched erythrocyte ghosts, although they did not conclude that poly(C9) necessarily traverses completely the protoplasmic leaflet.

It should be remembered that poly(C9) is not required for any of the known cytolytic functions of complement (Dankert & Esser, 1985, 1987). Thus, the transmembrane orientation of the MAC cannot be used to refute the leaky-patch model or support the doughnut model of MAC action. According to the leaky-patch hypothesis, the MAC interacts with and reorganizes lipids in its immediate environment in such a way as to break locally the membrane's permeability barrier. In previous spin-labeling studies it was shown by Esser et al. that complement proteins C5b-8 and C5b-9 do alter the order of lipids in planar membranes (Esser et al., 1979b), although the structural correlate of that reordering was not identified. Conceivably, the lipid areolas that we observed surrounding single C5b-9 complexes represent that correlate, and they could be evidence of a "leaky patch".

In weighing this possibility, one must consider whether such features are artifacts of the experimental procedure. Plastic deformation of the bilayer in a region surrounding the C5b-9 complex prior to actual fracture might produce a raised region on the EF like those shown in Figure 6. But it should also produce a raised region on the PF, where depressed regions were found. Sunken areas were sometimes found surrounding ES doughnuts on parts of the membrane that had not been fractured (e.g., Figure 4). It therefore seems unlikely that plastic distortion of the membrane generated the patches surrounding C5b-9 complexes. Could the process of etching per se create the lipid patches? Fracturing creates 17-nm holes in the PF, which could allow fairly rapid sublimation of water during the etch period. Consequent loss of the ice beneath the membrane might then cause the membrane to sag, accounting for the depressions seen about the PF holes. However, this rationale fails to explain the presence of raised areas on the EF, areas which roughly match in size the depressed regions on the ES. On the basis of these arguments it appears that the lipid islands are not artifacts of fracture or etching.

What evidence is there on the physical–chemical nature of the complement-induced patches? Periodic ripples characteristic of the $P_{\beta'}$ lipid phase traveled straight through some of them, indicating that they were composed primarily of lipid organized as a bilayer.[2] From the average patch diameter of

61 nm one may calculate that, after correction for the area of the MAC itself, the patches probably contained the equivalent of 4900–5600 molecules of solid-phase DPPC per monolayer (48 Å^2/molecule). In contrast, a boundary layer of DPPC (Jost et al., 1973) surrounding the MAC would contain only about 65–110 molecules per monolayer. To our knowledge no comparable long-range effect has been reported for other integral proteins. Two plausible hypotheses come to mind that might account for the altered surface curvature existing around C5b-9 complexes.

First, poly(C9) may have associated with it some peripheral protein, perhaps rearranged C5b-8, that binds to one of the classes of lipid present, resulting in head-group compaction and the observed bilayer warping. It is pertinent that binding of polylysine to the outer surface of vesicles containing negatively charged lipid results in formation of patches (Hartmann et al., 1977) reminiscent of those we found on C5b-9-treated vesicles. Second, poly(C9) may induce local accumulation of one of the minor lipid components. For example, the carbohydrate moieties situated at either end of poly(C9) (DiScipio & Hugli, 1985) might interact with the carbohydrates of DNP gangliosides. Previous freeze–fracture studies indicate that certain gangliosides form clusters in vesicles composed of synthetic lipids (Tillack et al., 1982), and spin-label data suggest that glycophorin may facilitate this process (Sharom & Grant, 1978). Whatever the origin of the patches is, it must encompass the observation that not all of the C5b-9 complexes seem to induce patch formation (see, e.g., Figure 4).

In summary, our most notable finding was that the C5b-9 complex is capable of causing a strikingly long-range alteration in the surface curvature of the bilayer. The exact nature of this perturbation remains unclear, although it does not seem to be an artifact of fracture or etching. The C5b-9-induced lipid patches may or may not be involved in complement function. Beyond this possibility, an understanding of how the patches are generated may yield insight into the chemistry of protein–lipid interaction in biological membranes.

ACKNOWLEDGMENTS

We gratefully acknowledge the initial contributions of Dr. K. P. Leung to this work.

Registry No. C5b-8, 82903-91-1; C5b-9, 82986-89-8.

REFERENCES

Bhakdi, S., Speth, V., Knufermann, H., Wallach, D. F. H., & Fischer, H. (1974) *Biochim. Biophys. Acta 356*, 300–308.

Cheng, K.-H., Wiedmer, T., & Sims, P. J. (1985) *J. Immunol. 135*, 459–464.

Dankert, J. R., & Esser, A. F. (1985) *Proc. Natl. Acad. Sci. U.S.A. 82*, 2128–2132.

Dankert, J. R., & Esser, A. F. (1987) *Biochem. J. 244*, 393–399.

Dankert, J. R., Shiver, J. W., & Esser, A. F. (1985) *Biochemistry 24*, 2754–2762.

da Silva, P. P., & Kan, F. W. K. (1984) *J. Cell Biol. 99*, 1156–1161.

DiScipio, R. G., & Hugli, T. E. (1985) *J. Biol. Chem. 260*, 14802–14809.

Esser, A. F., & Sodetz, J. M. (1988) *Methods Enzymol.* (in press).

Esser, A. F., Bartholomew, R. M., Jensen, F. C., & Muller-Eberhard, H. J. (1979a) *Proc. Natl. Acad. Sci. U.S.A. 76*, 5843–5847.

Esser, A. F., Kolb, W. P., Podack, E. R., & Muller-Eberhard, H. (1979b) *Proc. Natl. Acad. Sci. U.S.A. 76*, 1410–1414.

Fairclough, R. H., Finer-Moore, J., Love, R. A., Kristofferson, D., Desmeules, P. J., & Stroud, R. M. (1983) *Cold Spring Harbor Symp. Quant. Biol. 48*, 9–20.

Gotze, O., Haupt, I., & Fischer, H. (1968) *Nature (London) 217*, 1165–1167.

Hartmann, W., Galla, H.-J., & Sackmann, E. (1977) *FEBS Lett. 78*, 169–172.

Haxby, J. A., Gotze, O., Muller-Eberhard, H. J., & Kinsky, S. C. (1969) *Proc. Natl. Acad. Sci. U.S.A. 64*, 290–295.

Hesketh, T. R., Dourmashkin, R. R., Payne, S. N., Humphrey, J. H., & Lachmann, P. J. (1971) *Nature (London) 233*, 620–623.

Hu, V. W., Esser, A. F., Podack, E. R., & Wisnieski, B. J. (1981) *J. Immunol. 127*, 380–386.

Iles, G. H., Seeman, P., Naylor, D., & Cinader, B. (1973) *J. Cell Biol. 56*, 528–539.

Kinsky, S. C. (1972) *Biochim. Biophys. Acta 265*, 1–23.

Lachmann, P. J., Munn, E. A., & Weissmann, G. (1970) *Immunology 19*, 983–986.

Luzzati, V., & Tardieu, A. (1974) *Annu. Rev. Phys. Chem. 25*, 79–94.

Mayer, M. M. (1972) *Proc. Natl. Acad. Sci. U.S.A. 69*, 2954–2958.

McCloskey, M. A., & Poo, M. (1986) *J. Cell Biol. 102*, 2185–2196.

McCloskey, M. A., Dankert, J. R., & Esser, A. F. (1986) *Fed. Proc., Fed. Am. Soc. Exp. Biol. 45*, 1941.

Podack, E. R., & Tschopp, J. (1982) *Proc. Natl. Acad. Sci. U.S.A. 79*, 574–578.

Podack, E. R., Esser, A. F., Biesecker, G., & Muller-Eberhard, H. J. (1980) *J. Exp. Med. 151*, 301–313.

Podack, E. R., Stoffel, W., Esser, A. F., & Muller-Eberhard, H. J. (1981) *Proc. Natl. Acad. Sci. U.S.A. 78*, 4544–4548.

Rash, J. E., & Hudson, C. S., Eds. (1979) *Freeze–Fracture: Methods, Artifacts, and Interpretations*, Raven, New York.

Reeves, J. P., & Dowben, R. M. (1969) *J. Cell. Physiol. 73*, 49–60.

Sharom, F. J., & Grant, C. W. M. (1978) *Biochim. Biophys. Acta 507*, 280–293.

Sims, P. J. (1984) *Biochemistry 23*, 3248–3260.

Steckel, E. W., Welbaum, B. E., & Sodetz, J. M. (1983) *J. Biol. Chem. 258*, 4318–4324.

Stolfi, R. L. (1968) *J. Immunol. 100*, 46–54.

Szoka, F., Olson, F., Heath, T., Vail, W., Mayhew, E., & Papahadjopoulos, D. (1980) *Biochim. Biophys. Acta 601*, 559–571.

Tillack, T. W., Wong, M., Allietta, M., & Thompson, T. E. (1982) *Biochim. Biophys. Acta 691*, 261–273.

Tranum-Jensen, J., & Bhakdi, S. (1983) *J. Cell Biol. 97*, 618–626.

Tschopp, J., Muller-Eberhard, H. J., & Podack, E. R. (1982) *Nature (London) 298*, 534–538.

Tschopp, J. Engel, A., & Podack, E. R. (1984) *J. Biol. Chem. 259*, 1922–1928.